JTTEE5 20:154–159
DOI: 10.1007/s11666-010-9598-5
1059-9630/$19.00 © ASM International



# The Structure and Properties of Plasma Sprayed Iron Oxide Doped Manganese Cobalt Oxide Spinel Coatings for SOFC Metallic Interconnectors

*Jouni Puranen, Juha Lagerbom, Leo Hyvärinen, Mikko Kylmälahti, Olli Himanen, Mikko Pihlatie, Jari Kiviaho, and Petri Vuoristo*

*(Submitted May 14, 2010; in revised form October 28, 2010)*

**Manganese cobalt oxide spinel doped with $Fe_2O_3$ was studied as a protective coating on ferritic stainless steel interconnects. Chromium alloying causes problems at high operation temperatures in such oxidizing conditions where chromium compounds evaporate and poison the cathode active area, causing the degradation of the solid oxide fuel cell. In order to prevent chromium evaporation, these interconnectors need a protective coating to block the chromium evaporation and to maintain an adequate electrical conductivity. Thermal spraying is regarded as a promising way to produce dense and protective layers. In the present work, the ceramic Mn-Co-Fe oxide spinel coatings were produced by using the atmospheric plasma spray process. Coatings with low thickness and low amount of porosity were produced by optimizing deposition conditions. The original spinel structure decomposed because of the fast transformation of solid-liquid-solid states but was partially restored by using post-annealing treatment.**

**Keywords** interconnect, Mn-Co spinel, plasma spraying, SOFC

## 1. Introduction

Interconnectors (ICs) are used in a solid oxide fuel cell (SOFC) to provide an even fuel and oxidant distribution through a cell construction, to prevent fuel and oxygen gases from mixing and to connect the cells electrically in series. Traditional IC materials used in the electrolyte-supported cells, where operating temperatures were above 800 °C, were mainly alloyed lanthanum chromites (Ref 1, 2). By using the anode-supported cells, it is possible to use a thinner electrolyte layer and in this way decrease the SOFC operating temperature under 800 °C. Lower operating temperatures give the advance of using new material alternatives. These have been developed in order to obtain better electrical properties and especially to lower manufacturing costs when designing co-, cross- and counterflow gas channel configurations. Potential materials for this use are chromium-based alloys, for example, ferritic stainless steels. Chromium alloying gives good corrosion protection and moderate corrosion resistance at high operating temperatures (600-800 °C) and in highly oxidizing environments (Ref 2).

The corrosion protection is based on the forming of $Cr_2O_3$ scale on the steel surface. Chromium oxide tends to have low electrical resistivity at elevated temperatures ($1 \times 10^2$ Ω/cm at 800 °C) and by alloying other elements, for example, manganese, the formed oxide layer properties can be modified (Ref 2-4). The risk of using high chromium alloyed steels is the forming and the evaporation of chromium trioxide $CrO_3$ and chromium hydroxides $CrO_2(OH)_2$, depending on the cathode side inlet atmosphere. These compounds may transfer to a cathode active area (triple phase boundary, TPB), the area where oxygen is able to ionize. Compounds reduce back to $Cr_2O_3$ and cause the decreasing of the size of the active area causing a drop in the efficiency of the cell. This process is called chromium poisoning or degradation. The types of used cathode materials have an effect on the degradation speed. Some previous studies have reported that especially cathodes with higher amount of Sr alloying (La-Sr-Co-Fe, La-Sr-Fe, and La-Sr-Mn) suffer the most Cr-poisoning effect. One possible reason for this is that Sr reacts with Cr

This article is an invited paper selected from presentations at the 2010 International Thermal Spray Conference and has been expanded from the original presentation. It is simultaneously published in *Thermal Spray: Global Solutions for Future Applications, Proceedings of the 2010 International Thermal Spray Conference*, Singapore, May 3-5, 2010, Basil R. Marple, Arvind Agarwal, Margaret M. Hyland, Yuk-Chiu Lau, Chang-Jiu Li, Rogerio S. Lima, and Ghislain Montavon, Ed., ASM International, Materials Park, OH, 2011.

**Jouni Puranen, Leo Hyvärinen, Mikko Kylmälahti,** and **Petri Vuoristo**, Department of Materials Science, Tampere University of Technology, Tampere, Finland; **Juha Lagerbom**, VTT, Research Centre of Finland, Tampere, Finland; and **Olli Himanen, Mikko Pihlatie,** and **Jari Kiviaho**, VTT, Research Centre of Finland, Espoo, Finland. Contact e-mail: jouni.puranen@tut.fi.

and forms the $SrCrO_4$ phase. Degradation speed was the lowest when used cathode materials did not contain any Sr alloying, for example, La-Ni-Fe (Ref 5-7).

The protective coatings are used in order to minimize the oxidation of the IC and to prevent the evaporation of chromium compounds. Ensuring long-term usability, the coatings must fulfill the following requirements: (i) an excellent electrical conductivity with the objective of 100% electronic conduction so the effect of ohmic losses does not negatively affect the power density of the stack; (ii) a good chemical, microstructural, and phase stability at the stack operating temperature in an oxidizing environment; (iii) the coefficient of thermal expansion (CTE) of the coating should be near the other stack components such as the metallic IC and the cathode; (iv) a thermal conductivity at the lowest limit of 5 W/m/K at the point when generated heat from the cathode is transferred to the anode for endothermic fuel reformation reactions; and (v) the coatings together with the metallic substrate should have high temperature strength and creep resistance and provide structural support when used as a stationary and an auxiliary power unit under external stresses and vibrations (Ref 2).

The coating materials that have been previously studied as protective coatings are mainly the so-called perovskite materials with a chemical structure of $(AB)_2O_3$, where A and B are metallic cations. The most used materials have been lanthanum-manganese oxides (Ref 8-12) and lanthanum-cobalt/chromium oxides (Ref 3, 9, 12-18) with selected alloying, mainly in order to modify electrical and diffusion barrier properties. The use of these coatings is based on the same kind of composition and crystal structure as in the cathode materials. The coatings and the cathode have the same kind of mechanical behavior in elevated temperatures. The main difference between the cathode and the protective coating is that whereas the cathode layer is porous the protective coating needs to be dense to prevent the evaporation of harmful chromium compounds and oxidation of the substrate. Thermal spraying (Ref 8-16, 18) and spin coating (Ref 17) are used as a fabrication method. The main problem in all studies still seems to be manufacturing dense and thin coating structures so that the oxidation of substrate materials can fully be eliminated in long-time exposure.

An interesting alternative for perovskite are materials with a spinel structure, $(AB)_3O_4$, where A and B are metallic cations. Some previous studies have been published where spinel materials with a composition of manganese-cobalt oxides (Ref 3, 12, 19-21) and manganese-chromium oxides (Ref 20) have been used as the protective coating layer against the evaporation of harmful chromium compounds, working as an active layer forming more stable chromium oxide compounds. Larring et al. (Ref 12) found in their experiments that $(Mn,Co)_3O_4$ spinel worked effectively as a chromium barrier, even when compared with often used perovskite materials. They also discovered that the mechanical properties of the coating seem to match the used substrate alloy. When using iron (Fe) doped manganese-cobalt oxide spinel, it is possible to improve the electrical and mechanical properties of the coating. Studies have shown that a proper amount of Fe in $MnCo_{2-x}Fe_xO_4$ is in the range of $0.1 < x < 0.25$ (Ref 22). The spinel coatings are mainly manufactured by slurry painting/spraying (Ref 12, 19-21), physical vapor deposition (Ref 23), and DC electrodeposition methods (Ref 24) but there are no studies where Mn-Co spinel, especially with Fe alloying, are being manufactured by thermal spaying. In this article, the suitability of atmospheric plasma spraying (APS) is being studied as a fast manufacturing method for producing thin, under 50 μm thick, protective coatings for thin 0.2 mm ferritic stainless steel substrates.

## 2. Experimental

### 2.1 Powder Manufacturing

$Fe_2O_3$ doped Mn-Co spinel powder was produced by solid state synthesis and agglomerated to spherical form by spray drying. $MnCo_{1.8}Fe_{0.2}O_4$ (MCF) powder was prepared by weighing appropriate amounts of $MnCO_3$, $CoCO_3$, and $Fe_2O_3$ powders together and milling them for 20 h in a drum ball mill. After the milling, the mixture was calcinated at 1000 °C in air for 6 h to obtain the spinel structure. The powder was dispersed in water using 1 wt.% of dispersant (Dispex A40, Ciba, Basel, Switzerland) by a planetary ball mill, 2 h at 300 rpm with $ZrO_2$ balls (Fritsch pulverisette 5, Fritsch GmbH, Germany). 2 wt.% of bonding agent (PVA, Celanese, Dallas) was added to the slurry by a high shear mixer. The suspension was spray dried by spray dryer (Niro pilot, GEA Niro, Soeborg, Denmark). A rotary nozzle with high rotation speed was used in order to get the fine agglomerate size needed for thin coating production. The powder was sintered at 1150 °C to improve powder strength, where an isothermal step at 500 °C for 2 h was used in order to pyrolyze the PVA without fracturing the agglomerates. After sintering, the powder was sieved. Particle size of $-29 + 13$ μm (d90-d10) was measured by laser diffraction sensor (Helos, Sympatec GmbH, Clausthal-Zellerfeld, Germany).

### 2.2 Coating Manufacturing

The coatings were produced by using a plasma gun (F4-MB, Sulzer Metco, Winterthur, Switzerland). Parameters were selected so that the influence of the used gun power on coating properties could be studied. The lowest energy parameter at which a stable coating could be produced was selected to be as parameter P1. More detailed parameters can be seen in Fig. 1. Constant spraying distance (120 mm) and surface speed were assured by using an X-Y manipulator. The desired average coating thickness was about 15-20 μm.

Samples sprayed with parameters 1, 7, and 9 were annealed to examine the restoring of the spinel structure. The samples were annealed at 800 °C for 3 h at normal atmosphere and the crystal structure was then analyzed. By choosing samples 1, 7, and 9 the influence of gun power could be estimated.

The substrate material was ThyssenKrupp VDM Crofer 22 APU specially tailored for SOFC use (Cr: 20-24 wt.%). The thickness of the substrate was 0.2 mm with 70 × 70 mm outer dimensions. The substrates were grit blasted (240 grit $Al_2O_3$) before plasma spraying so that the needed adhesion could be reached. Grit blasting was performed to both sides to avoid the bending of the thin substrate. After being plasma sprayed, the samples were laser cut to 15 × 20 mm pieces. The pieces were then molded in cold resin in a chamber under reduced pressure to prevent cracking and to give the samples an extra support while grinding and polishing.

### 2.3 Characterization Methods

The powder and the coatings were analyzed by using a scanning electron microscope (SEM) (Philips XL 30, Philips, Amsterdam, Netherlands). Secondary electron (SE) and back-scattering electron (BSE) modes were used for morphological inspections and energy dispersed spectroscopy (EDS) mode was used for quantitative analysis of the elements. Porosity values were calculated by using an image analysis tool. Qualitative phase analysis of the powder and as-sprayed and annealed coatings was performed by using a x-ray diffractometer using Cu-$K_\alpha$ radiation source (Siemens D-500, Siemens, Berlin, Germany).

Hardness tests were performed by using a microhardness tester (MMT-X7, Matsuzawa, Akita, Japan). The hardness values were measured using a 250 mN cell load. Using this extraordinarily low test load, it was ensured that an indentation mark did not extend outside of the coatings' cross-section area. Results are the average values of five separate measurements.

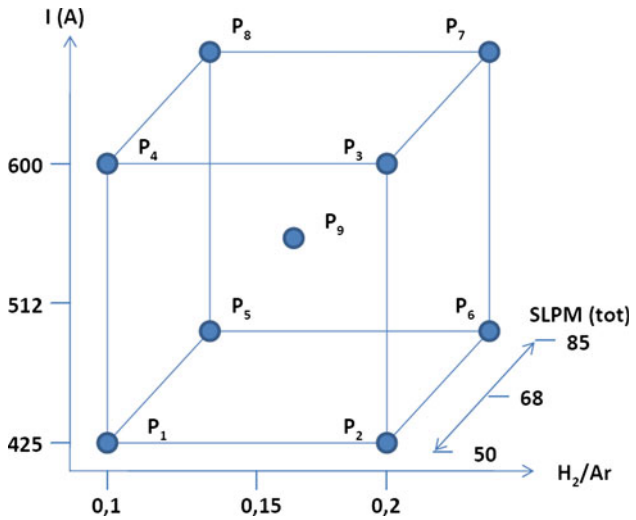


**Fig. 1** Plasma spraying parameters

## 3. Results and Discussion

### 3.1 Powder Characterization

The powder morphology is presented in Fig. 2. The particles were spherical because of spray drying and formed of primary particles of the size of 2-3 μm which can be seen from a cross-sectional SEM image. Some particles were attached to each other which affected flow properties negatively in a powder feeder, but the powder was still sprayable. When the chemical composition of the powder was analyzed, the amount of Fe seemed to be higher than it should be (Table 1). The calculated amount of Fe was 6.7%, but the analyzed value was 12.4%.

**Table 1 Amount of elements in atomic percentages (at.%) (EDS)**

| Elements | Powder | P1 | P2 | P3 | P4 |
|---|---|---|---|---|---|
| Mn (33.3) | 31.3 | 30.5 | 31.4 | 32.0 | 31.0 |
| Fe (6.7) | 12.4 | 11.9 | 12.2 | 13.0 | 12.2 |
| Co (60) | 56.3 | 57.6 | 56.4 | 55.4 | 56.8 |

| | P5 | P6 | P7 | P8 | P9 |
|---|---|---|---|---|---|
| Mn | 29.3 | 30.7 | 31.2 | 30.0 | 30.4 |
| Fe | 12.5 | 11.7 | 12.0 | 11.7 | 11.7 |
| Co | 58.1 | 57.6 | 56.9 | 58.3 | 58.0 |

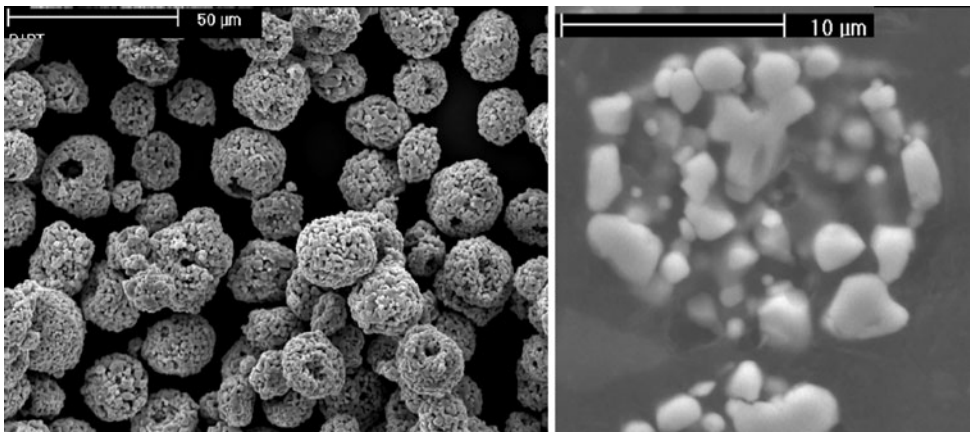


**Fig. 2** Secondary electron image (SEM) of MCF-spinel powder (left). Cross-sectional secondary electron image (SEM) of MCF-spinel powder (right)

The amount was probably altered because Fe-$K_\alpha$ radiation was at the same value when compared to manganese-$K_\beta$ radiation and Fe-$K_\beta$ radiation was at the same value compared to cobalt-$K_\alpha$ radiation. Overlapping of radiation peaks increases the values, even though the mixture ratios were correct when the powder was manufactured.

### 3.2 Coating Structural Characterization

The coatings (Fig. 3) had a typical plasma-sprayed structure. In all the coatings, some pores, cracks and some large pull-outs were present. Clear boundaries in separate spraying layers were not present. The desired coating thickness was achieved with a relatively dense microstructure with small variations of porosity (Table 2). The coatings had a good adhesion to the substrate and no visible cracking on the interface, but in some coatings vertical cracks were present, especially in the coatings where high energy parameters were used. This might be the result of small differences in CTE values. For $MnCo_{1.8}Fe_{0.2}O_4$ sintered at 1000 °C the CTE value is $12.3 \times 10^{-6}$/K (Ref 22) and for Crofer 22 APU depending on the temperature while spraying it, the CTE values varies (200-1000 °C) 10.3-12.7 $\times 10^{-6}$/K (Ref 25). These cracks may offer a pathway for oxygen access and chromium evaporation.

### 3.3 Coating Chemical and Phase Analysis

The influence of the spraying parameters on selective compound evaporation is presented in Table 1. Values have been calculated by analyzing the whole image area.

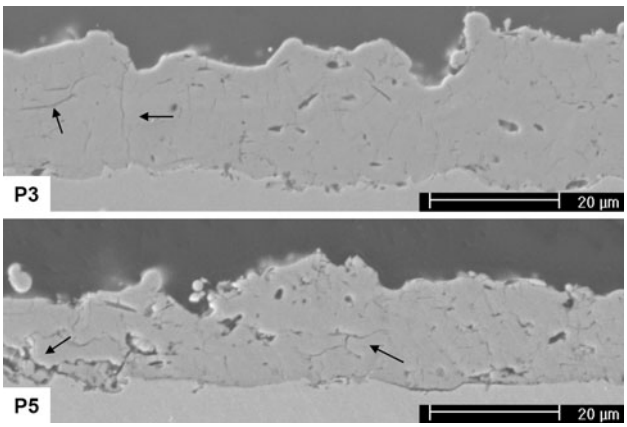


**Fig. 3** Cross-sectional secondary electron image (SEM) of plasma sprayed spinel coatings. Lowest porosity coating (P3) and highest porosity coating (P5)

**Table 2 Amount of porosity in percentages (%)**

| Parameter | Porosity, % | Parameter | Porosity, % |
|---|---|---|---|
| P1 | 6.1 | P6 | 6.6 |
| P2 | 5.3 | P7 | 5.7 |
| P3 | 3.8 | P8 | 5.3 |
| P4 | 5.7 | P9 | 6.7 |
| P5 | 6.9 | | |

When comparing EDS measurements with the values of the powder, significant alteration could not be noticed. In this case, the coating compositions were not altered, although high energetic spraying parameters were used. It is possible that the coatings include smaller areas where selective evaporation has occurred. The reason for this is the fluctuation of plasma flame/energy resulting in molten droplets with altered composition. Due to the same reason, a similar variation of Fe amount can be seen in EDS analysis as was observed in the powder's case.

When analyzing the crystal structures of the as-sprayed coatings (Fig. 4), it can be noticed that the original spinel structure is decomposed. Peaks in the coatings were analyzed to be near the FeO (wuestite) kind of structure with a cubic form. When comparing low energy spraying parameters with high energy parameters the peaks were equal, meaning that the variations of spraying parameters did not affect the formed crystal structure. The reason for the presented structure lies in the coating preparation method where material is melted and cooled rapidly. When droplets hit the substrate and metastable crystal structures, material decomposition occurs and new compositions are being formed.

The XRD results of pre-selected annealed samples (Fig. 5) reveal that the spinel structure can be restored by using a separate annealing. When comparing the coatings with the powder, it can be seen that small intensity peaks of $MnCo_{1.8}Fe_{0.2}O_4$ spinel are present. In sample P1 there is also a high intensity peak of Fe, which was the result of the reflection of the substrate material and can be neglected. In all the coatings, the peaks of an FeO kind of structure and $Co_3O_4$ spinel were also present. The peaks of FeO were a result of a situation where the restoring of the spinel structure was not fully completed and where it may need more time for a complete reformation reaction. The presence of $Co_3O_4$ spinel peaks was an interesting result. These peaks might be the result of the selective evaporation of those components which cannot be seen in the EDS analysis taken from the whole coating area.

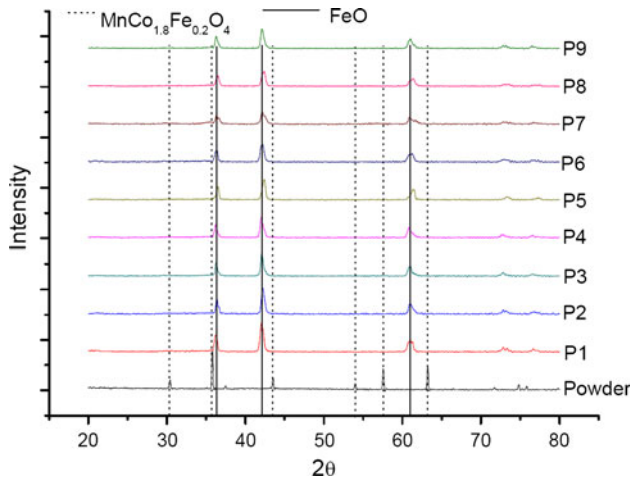


**Fig. 4** XRD-analysis of as-sprayed coatings with all spraying parameters

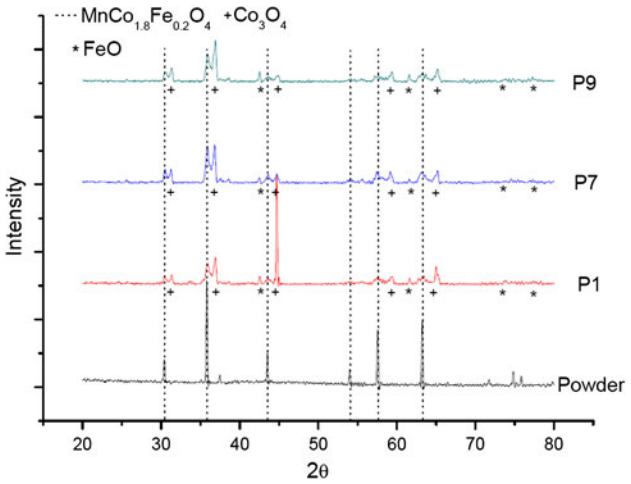


**Fig. 5** XRD analysis of selected annealed coatings

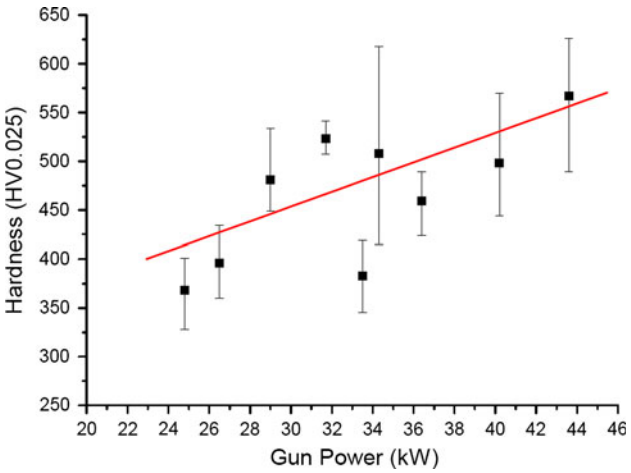


**Fig. 6** Hardness values related to used gun power

In this case, it may be that manganese was evaporated during spraying. The result of this was the metastable form of Mn-Co-Fe spinel, Fe oxide and an excess amount of cobalt in the form of cobalt oxide spinel. Lim et al. (Ref 11) got the same results of evaporation of manganese when plasma spraying perovskite structured $La_{0.8}Sr_{0.2}MnO_3$ on metallic ICs.

### 3.4 Coatings' Mechanical Properties

Hardnesses of the protective coatings varied from 320 to 600 $HV_{0.025}$. When plotting the hardness as a function of gun power (Fig. 6) and inspecting the interdependency fitting with linear regression ($R$ value 0.521), it can be seen that the hardness values are related to the used gun power. By increasing the used gun power by 80%, the coatings' hardness values increased by 35% on average.

The reason for the increased hardness values could be related to single splat behavior in the coating process. When low gun power was used the particles were not able to fully melt and, as a result, coatings contained partially melted particles. These particles have poor adhesion and degrade the internal strength of the coating. When the used gun power was increased, the single particles were able to melt more homogeneously and form a coating where un-melted particles were not present. The coating was then formed of splats with good adhesion, which may influence the crack networks between splats so that they are smaller compared to the coatings prepared by using low gun power. In this case, the use of high energy parameters is an advantage that could provide a coating which provides better protection against chromium evaporation from the substrate.

## 4. Conclusions

The spinel materials are an interesting option for protective coatings on ferritic stainless steels instead of perovskites that are already being used. Earlier studies in this area were based on manufacturing these coatings by slurry- or thin film techniques. In this study, APS has been used to produce Mn-Co-Fe spinel coating on the thin metallic IC in SOFCs.

The conventional plasma sprayed coating has always included some pores and cracks because of the nature of the spraying process. When plasma spraying Mn-Co-Fe spinel, the original $MnCo_{1.8}Fe_{0.2}O_4$ crystal structure seems to decompose in the fast changes of transformation (solid-liquid-solid) which leads to the forming of metastable compounds. Also some selective evaporation of the components, for example, manganese, can happen. The original spinel structure will decompose but it can be partially restored by using a separate annealing process. In this process, metastable phases will transform by diffusion and growth of grain size and form stable compositions, for example, $Co_3O_4$.

The mechanical properties of the coatings were highly dependent on the used spray parameters. By increasing the used gun power, a harder coating structure could be achieved and the amount of un-melted particles decreased. Negative influences of using high energy spraying parameters on coating composition in this research were not noticed.


## Acknowledgments

The authors would like to acknowledge Tekes—the Finnish Funding Agency for Technology and Innovation and a group of industrial partners of the SofcPower project for financial support.


## References


1. J. Jeffrey and W. Fergus, Lanthanum Chromite-Based Materials for Solid Oxide Fuel Cell Interconnects, *Solid State Ion.*, 2004, **171**, p 1-15
2. W.Z. Zhu and S.C. Deevi, Development of Interconnect Materials for Solid Oxide Fuel Cells, *Mater. Sci. Eng.*, 2003, **A348**, p 227-243

3. H. Kurokawa, P.Y. Hou, X. Chen, C. Jacobson, L. DeJonghe, and S.J. Visco, Effect of Protective Coatings for Alloy Interconnect on Oxidation and Cr Vaporization, *Materials Science and Technology*, Vol. 1, Materials and Systems, 2006, p 208-216
4. W.Z. Zhu and S.C. Deevi, Opportunity of Metallic Interconnects for Solid Oxide Fuel Cells: A Status on Contact Resistance, *Mater. Res. Bull.*, 2003, **38**, p 957-972
5. J.W. Fergus, Metallic Interconnects for Solid Oxide Fuel Cells, *Mater. Sci. Eng.*, 2005, **397**, p 271-283
6. F. Chen, E. Sun, J. Yamanis, J. Hawkes, J. Smeggil, S. Warrier, and J.-W Kim, Cr Poisoning Effect for Solid Oxide Fuel Cells, *Materials Science and Technology*, Vol. 1, Materials and Systems, 2006
7. J.Y. Kim, N.L. Canfield, L.A. Chick, K.D. Meinhardt, and V.L. Sprenkle, Chromium Poisoning Effects on Various Cathodes, *Ceram. Eng. Sci. Proc.*, 2008, **26**(4), p 129-138
8. H.W. Nie, T.L. Wen, and H.Y. Tu, Protection Coatings for Planar Solid Oxide Fuel Cell Interconnect Prepared by Plasma Spraying, *Mater. Res. Bull.*, 2003, **38**, p 1531-1536
9. J. Lagerbom, U. Kanerva, A.-P. Nikkilä, T. Varis, M. Kylmälahti, and P. Vuoristo, Phase Stability and Structure of Conductive Perovskite Ceramic Coatings by Thermal Spraying, *Proceedings of the International Thermal Spray Conference*, 2-4 June 2008 (Maastricht), CD-ROM
10. F. Changjing, S. Kening, and Z. Derui, Effects of $La_{0.8}Sr_{0.2}Mn(Fe)O_3$ Protective Coatings on SOFC Metallic Interconnects, *J. Rare Earths*, 2006, **24**, p 320-326
11. D.P. Lim, D.S. Lum, J.S. Oh, and I.W. Lyo, Influence of Post-Treatment on the Contact Resistance of Plasma-Sprayed $La_{0.8}Sr_{0.2}MnO_3$ Coatings on SOFC Metallic Interconnector, *Surf. Coat. Technol.*, 2005, **200**, p 1248-1251
12. Y. Larring and T. Norby, Spinel and Perovskite Functional Layers Between Plansee Metallic Interconnect (Cr-5 wt% Fe-1 wt% $Y_2O_3$) and Ceramic $(La_{0.85}Sr_{0.15})_{0.91}MnO_3$ Cathode Materials for Solid Oxide Fuel Cell, *J. Electrochem. Soc.*, 2000, **47**(9), p 3251-3256
13. E. Garcia and T.W Coyle, Thermal Spray Deposition of Fuel Cell Interconnect Material, *Proceedings of the International Thermal Spray Conference*, 15-18 May 2006 (Seattle), CD-ROM
14. S.D. Park, S. Kumar, S.C. Lee, and C. Lee, Effects of Silver Addition on Mechanical Properties of Plasma Sprayed SOFC Interconnect Layer, *J. Therm. Spray Technol.*, 2008, **17**, p 708-714
15. S.Y. Hwang, J.H. Kim, B.G. Seong, and H. Yang, SOFC Interconnect Coating Using HVOF Process, *Proceedings of the International Thermal Spray Conference*, 15-18 May 2006 (Seattle), CD-ROM
16. R.H. Henne, T. Franco, and R. Ruckdäschel, High Velocity DC-VPS for Diffusion Protecting Barrier Layer in SOFCs, *Proceedings of the International Thermal Spray Conference*, 15-18 May 2006 (Seattle), CD-ROM
17. K. Fujita, K. Ogasawara, Y. Matsuzaki, and T. Sakarai, Prevention of SOFC Cathode Degradation in Contact with Cr-Containing Alloy, *J. Power Sources*, 2004, **131**, p 261-269
18. W.J. Quadakkers, H. Greiner, M. Hänsel, A. Pattanaik, A.S. Khanna, and W. Malléner, Compatibility of Perovskite Contact Layers Between Cathode and Metallic Interconnector Plates of SOFCs, *Solid State Ion.*, 1996, **91**, p 66-67
19. Z. Yang, G. Xia, and J.W. Stevenson, $Mn_{1.5}Co_{1.5}O_4$ Spinel Protection Layers on Ferritic Stainless Steels for SOFC Interconnect Applications, *Electrochem. Solid State Lett.*, 2005, **8**(3), p 168-170
20. X. Chen, P.Y. Hou, C.P. Jacobson, S.T. Visco, and L.C. De Jonghe, Protective Coatings on Stainless Steel Interconnect for SOFCs: Oxidation Kinetics and Electrical Properties, *Solid State Ion.*, 2005, **176**, p 425-433
21. Z. Yang, G.-G. Xia, X.-H. Li, and J.W. Stevenson $(Mn, Co)_3O_4$ Spinel Coatings on Ferritic Stainless Steels for SOFC Interconnect Applications, *Int. J. Hydrogen Energy*, 2007, **32**, p 3648-3654
22. T. Kiefer, M. Zahid, F. Tietz, D. Stöver, and H.-R. Zerfass, Electrical Conductivity and Thermal Expansion Coefficients of Spinel in the Series $MnCo_{2-x}Fe_xO_4$ for Application as a Protective Layer in SOFC, *Proceedings of the 26th Riso International Symposium on Materials Science*, Denmark, Roskilde, 2005
23. P.E. Gannona, V.I. Gorokhovsky, M.C. Deibert, R.J. Smith, A. Kayani, P.T. White, S. Sofie, Z. Yang, D. McCready, S. Visco, C. Jacobson, and H. Kurokawa, Enabling Inexpensive Metallic Alloys as SOFC Interconnects: An Investigation into Hybrid Coating Technologies to Deposit Nanocomposite Functional Coatings on Ferritic Stainless Steels, *Int. J. Hydrogen Energy*, 2007, **32**, p 3672-3681
24. J. Wu, Y. Jiang, C. Johnson, and X. Liu, DC Electrodeposition of Mn-Co Alloys on Stainless Steels for SOFC Interconnect Application, *J. Power Sources*, 2008, **177**, p 376-385
25. Material Data Sheet No. 4046 for Crofer 22 APU, ThyssenKrupp VDM